(Received 6 October 2023, Accepted 23 February 2024, Scheduled 1 March 2024)

Compact UWB Wearable Textile Antenna for On-Body WBAN Applications

Anju Maria* and Palayyan Mythili

Cochin University of Science and Technology, Cochin, Kerala, India

ABSTRACT: Wearable textile antennas have obtained remarkable attention in various medical fields due to their ease of integration and flexibility. This paper puts forward an Ultra Wide Band (UWB) Compact Textile Wearable Antenna (CTWA) for Wireless Body Area Network (WBAN) applications. The proposed antenna is a semicircular slotted elliptical antenna with an L-shaped stub and a partial defected ground plane. The antenna is fabricated on denim jeans ($\epsilon_r = 1.77$) and has an overall dimension of $27 \times 28 \times 0.7$ mm with an operating frequency range 3.01–15.98 GHz, radiation efficiency of 83.5–90.11%, and maximum gain of 5.81 dBi. Structural deformation studies including human body loading of the antenna are carried out, and the performance of the antenna is found to be stable. The proposed antenna has a low profile and high fractional bandwidth (137%) compared to the UWB wearable antennas reported in the literature. The calculated Specific Absorption Rate (SAR) of the antenna at the frequencies 4,7 and 10 GHz are 1.2, 1.06, and 1.58 W/Kg, respectively, which lies within the FCC (Federal Communications Commission) standard. The proposed CTWA is compact, flexible, wearable, and robust, which makes it suitable for on-body WBAN applications.

1. INTRODUCTION

In the recent times, there is significant advancement in the area of WBAN with the evolution of wearable technology. WBAN has numerous applications in the field of medicine, defence, emergency services, consumer electronics, etc. [1]. The applications of WBAN particularly in the medical field are real time patient care, remote health monitoring, microwave imaging, etc. A WBAN system comprises a network containing various nodes equipped with bio-sensors, motion detectors, and antennas for wireless connectivity. These nodes are placed either on the body or inside the body to measure bio-signals. The body centric wireless communication systems are classified into on-body and off-body communication systems. In the case of an on-body communication system, communication takes place between the antennas mounted on the sensor nodes located on the body of the same person. Similarly, in the case of an off-body communication system, the communication takes place between the antenna mounted on the sensor node located on the body of a person and the antenna at the base unit/mobile device in the surrounding environment [2]. Thus, the antenna is a key component that determines the quality of the wireless links in a WBAN system. For a distortion less transmission and reception of signals, the antennas used should be light in weight, robust, conformal, and compact with high radiation efficiency. Wearable antennas are widely accepted in the academia and industry since the future generation of wearable electronics demands the placement of antenna directly on the human body [3]. Wearable antennas are best suited for WBAN applications due to their advantages like compactness, low manufacturing cost, low fabrication complexity, flexibility, and integrability. A WBAN system mainly uses the high gain, low cost, and low power UWB (3.1–10.6 GHz) technology released by the Federal Communication Commission (FCC) in 2002 [4]. Wearable antennas are broadly classified into two, namely flexible antennas and textile antennas.

Flexible antennas as the name suggests use soft inexpensive flexible substrates like polymide, poly carbonate, poly dimethyl siloxane, polyethylene, liquid crystal polymer, etc. [5]. Some of the flexible antennas available in the literature are printed dipole antenna using polyimide substrate [6], elliptical monopole antenna using kapton substrate [7], microstrip patch antenna using rubber substrate [8], monopole antenna using polyimide substrate [9], fractal antenna using vinyl polymer substrate [10], microstrip patch antenna using liquid crystal polymer [11], etc. The bandwidth of these antennas were narrow, even though they were light in weight. Moreover, these flexible antennas cannot be directly integrated into the clothing which limits its application in medical and military fields [12].

On the other hand, textile antennas are antennas that are fabricated on the commonly available textile substrates like felt, cotton, jeans, silk, condura, etc. Among the textile substrates, denim jeans were found to be long lasting, strong, absorbing, and tear resistant. Compared with flexible antennas, they provide wide bandwidth, compactness, integrability, and low surface wave losses. This is due to the low dielectric value of the textile substrates which is usually less than three [13]. Owing to these facts, textile antennas are best suited for UWB-WBANs. Some of the applications of UWB textile antennas are

* Corresponding author: Anju Maria (anjumaria@cusat.ac.in).

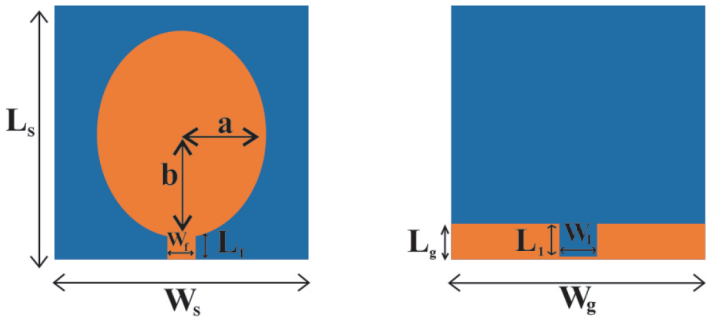

FIGURE 1. Top and bottom view of the simple elliptical monopole antenna.

medical imaging, location tracking, patient movement, capsule endoscopy, activity classification, etc. [14]. Several wearable UWB textile antennas like hexagon-shaped antenna on a cotton cloth [15], octagon-shaped antenna on a felt substrate [16], eye-shaped textile antenna on a denim substrate [17], hexagon-shaped antenna on a dacron substrate [18], rectangular patch antenna on a jute substrate [19], T-shaped antenna on a cotton substrate, etc. [20] have been reported in the literature. Though these antennas were highly flexible and easily integrable, their size was large. One of the important requirements of WBANs is to have an antenna with wider bandwidth. In [21], De et al. depicted that the partial ground plane antennas exhibit broader bandwidth, and in [22] Raj et al. showed that antennas with defected ground plane structures like slotted ground plane have a wider bandwidth.

For developing an efficient WBAN system, a flexible wearable antenna that performs well and is easily integratable on clothing is required. As the human body is a lossy medium, the antennas operating in the vicinity of a human body will suffer from electromagnetic distortions. The characteristics of the transmitting and receiving antennas like radiation pattern, S parameters, gain, and efficiency need to be evaluated when the antenna is placed on the lossy human body. In addition to this, the antenna's performance should not vary with the wearer's morphology or the location of the antenna [23]. In the same way, the electromagnetic radiations from the antenna can affect the human body. SAR is an important factor to measure the amount of electromagnetic radiation absorbed per unit mass by a human body. Hence, the antennas used for WBAN applications must possess a low SAR. There are two standards for SAR measurements, namely FCC (Federal Communications Commission) standard and IEC (International Electrotechnical Commission) standard. SAR limit is 1.6 W/Kg for 1 gram and 2 W/Kg for 10 gram in the case of FCC and IEC standards, respectively. Unlike conventional rigid antennas, textile antennas are subjected to concave and convex structural deformations when being placed on different parts of the human body. In [24, 25], textile antennas for on-body communications were put forward along with the structural deformation studies and SAR analysis. In these works, the antenna size was the limitation. Reducing the size of the antenna has always been a challenging task. An efficient textile antenna, for on-body WBAN applications, should be compact with high gain, broad bandwidth, low SAR, and low performance degradation with omnidirectional pattern.

In this paper, a compact UWB wearable textile antenna made of jeans material operating in the frequency band 3.01–15.98 GHz with large fractional bandwidth and high radiation efficiency is reported. The paper is organised as follows. Section 2 discusses the evolution of CTWA and its analysis. Section 3 presents the fabrication procedure of the CTWA, the measurement of reflection coefficients, radiation characteristics, gain, and efficiency of the proposed CTWA. In addition to this, the bending analysis, human body loading of the antenna, and the SAR analysis are performed. Finally, Section 4 draws the conclusion of the paper.

2. ANTENNA DESIGN

The proposed CTWA is a UWB monopole antenna. The CTWA is designed on a uniform and long lasting denim jeans substrate. The thickness of the substrate is measured using a screw gauge and is found to be 0.7 mm. The loss tangent ($\tan\delta$) of the chosen denim jeans substrate is 0.03034, and its permittivity (ϵ_r) is 1.77. The substrate is chosen as jeans since it is low in cost, flexible, strong, and easily integratable. Moreover, denim jeans are easily available and are a tear resistant textile material. Microstrip line feeding technique is adopted in this work. The merit of this feeding method is that it avoids spurious feed radiation and helps in achieving a wider bandwidth. The antennas are designed and simulated using CST microwave studio suite 2020.

2.1. Evolution of CTWA

The evolution of the UWB CTWA started by designing a simple elliptical monopole antenna on a denim jeans substrate. The substrate is of dimension $L_s \times W_s = 27 \times 28$ mm, where L_s is the length of the substrate, and W_s is the width of the substrate. The partial ground plane is of dimension ($L_g \times W_g$) 2×28 mm, where L_g is the length of the substrate, and W_g is the width of the substrate. An elliptical patch with semi major axis, a, and semi minor axis, b, is mounted on the top of the substrate. These dimensions were parametrically optimised using CST Microwave studio, and the optimum values are 12 and 9.5 mm, respectively. A 50 Ω microstrip feed line is employed. The feed is of dimension ($L_f \times W_f$) 2×3 mm, where

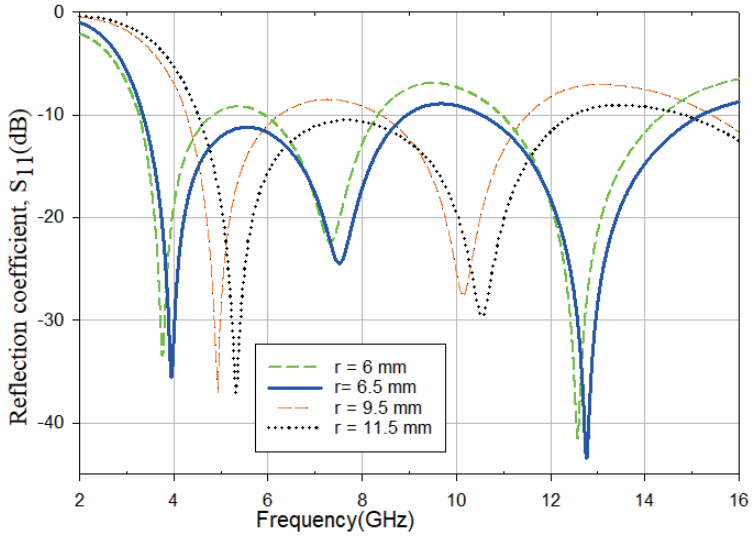

FIGURE 2. Parametric analysis — effect of slot radius.

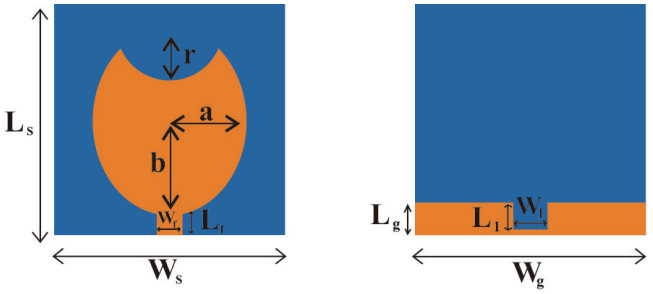

FIGURE 3. Top and bottom view of the semi circular slotted elliptical monopole antenna.

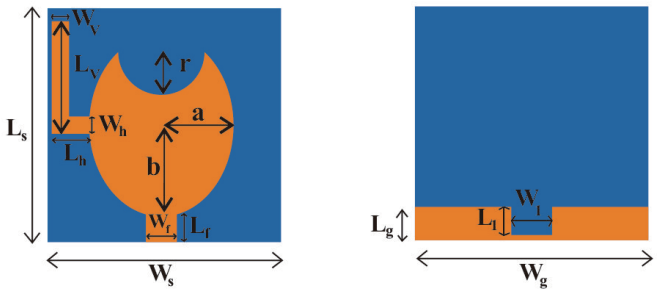

FIGURE 4. Top and bottom view of the semi circular slotted elliptical monopole with L stub (CTWA).

L_f is the length of the feed, and W_f is the width of the feed. A small rectangular slot parametrically optimised with dimension ($L_1 \times W_1$) 1.2×4 mm is introduced in the partial ground plane to increase the bandwidth. L_1 is the length of the slot, and W_1 is the width of the slot. The bandwidth of the antenna is from 3.23 to 15.4 GHz with a notch in the band from 7.96 to 10.3 GHz. Fig. 1 shows the layout of the simple elliptical monopole antenna with a rectangular slot in the ground plane (Antenna 1).

Since the achieved bandwidth did not cover the entire UWB, a semicircular slot is introduced in the patch for improving the bandwidth of the antenna [26]. The presence of this slot changes the current distribution of the patch, thereby improving the bandwidth. The parametric analyses for different slot positions are carried out, and the slot located at the top of the patch offers better results than other slot locations. Further, the dimensions of the semicircular slot are optimised parametrically and shown in Fig. 2. The slot with radius $r = 6.5$ mm provided better results. Fig. 3 depicts the layout of a semi-circular slotted elliptical monopole antenna (Antenna 2). This antenna has bandwidth of 3.29 to 15.06 GHz with a reduced notch in the band from 9 to 10.3 GHz. To eliminate the notch and to shift the lower frequency, an L-shaped stub [27] is introduced on the left side of the semi-circular slotted elliptical patch (Antenna 3/proposed CTWA) as shown in Fig. 4. The effect of stub height on the lower bound of the frequency is studied, and an optimum value of 15 mm is chosen. Fig. 5 shows the parametric analysis for different stub heights.

Table 1 shows the consolidated dimensions of the proposed CTWA. The horizontal strip is of length (L_h) 2.5 mm and width (W_h) 2 mm. The vertical strip is of length (L_v) 15 mm and width (W_v) 2 mm. The presence of the L-shaped stub resulted in achieving the entire UWB. The obtained bandwidth is from 3.01 to 15.8 GHz.

The simulated reflection coefficient characteristics of Antenna 1, Antenna 2, and Antenna 3 (proposed CTWA) are as shown in Fig. 6. From the simulated return loss characteristics it can be inferred that the proposed CTWA covers the entire UWB and has a bandwidth from 3.01 to 15.8 GHz. In order to understand the resonating features of the antenna, the surface current distributions of the CTWA at frequencies 3.2, 7, and 10.2 GHz are shown in Fig. 7. From the plot it can be inferred that the L-shaped stub is responsible for the shift in lower frequency.

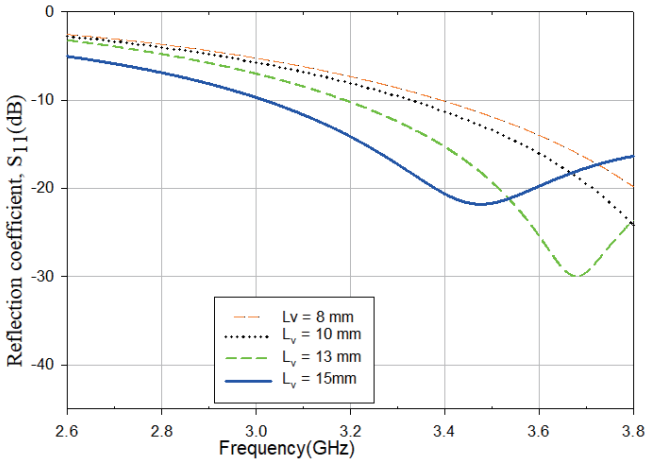

FIGURE 5. Parametric analysis — effect of stub height.

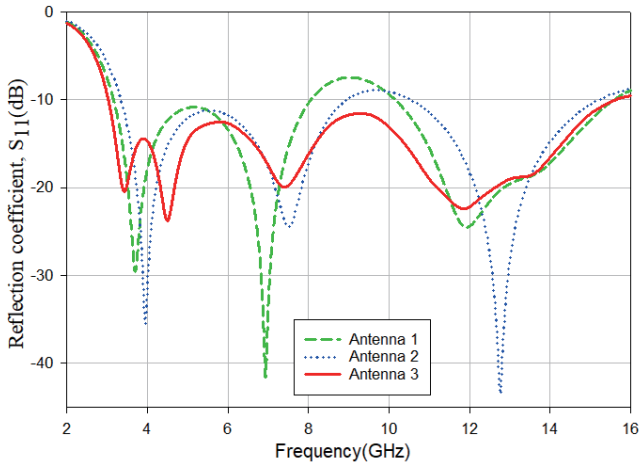

FIGURE 6. Reflection coefficient characteristics of Antenna 1, Antenna 2 and Antenna 3 (proposed CTWA).

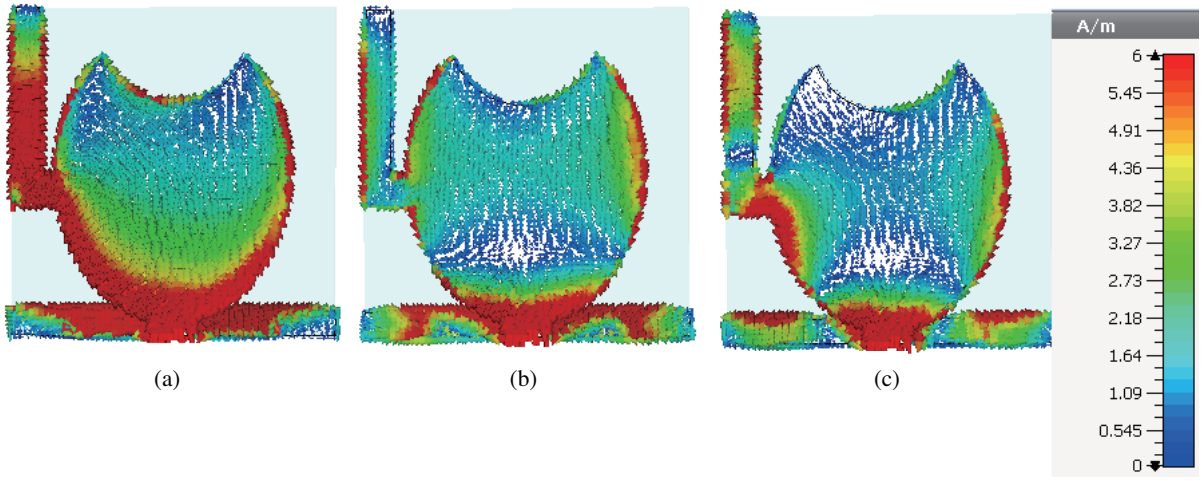

FIGURE 7. Surface current distribution of the proposed CTWA. (a) 3.2 GHz, (b) 7 GHz and (c) 10.2 GHz.

TABLE 1. Dimensions of the proposed CTWA.

Sl. No	Antenna parameter	dimensions (mm)
1	W_s (width of the substrate)	28
2	L_s (length of the substrate)	27
3	h (height of the substrate)	0.7
4	r (radius of the semicircular slot)	6.25
5	W_f (width of the feed)	3
6	L_f (length of the feed)	2.5
7	W_g (width of the ground)	28
8	L_g (length of the ground)	2
9	W_v (width of the vertical strip)	2
10	L_v (length of the vertical strip)	15
11	W_h (width of the horizontal strip)	2
12	L_h (length of the horizontal strip)	2.5
13	W_1 (width of the slot)	4
14	L_1 (length of the slot)	1.2

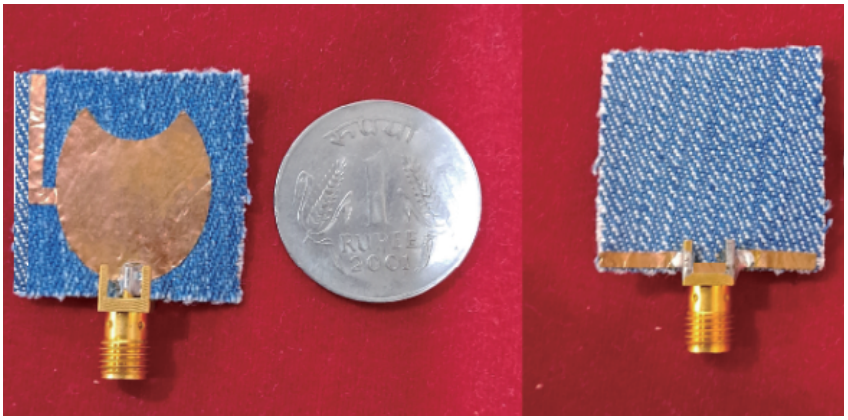

FIGURE 8. Fabricated prototype: Front and rear view of the CTWA.

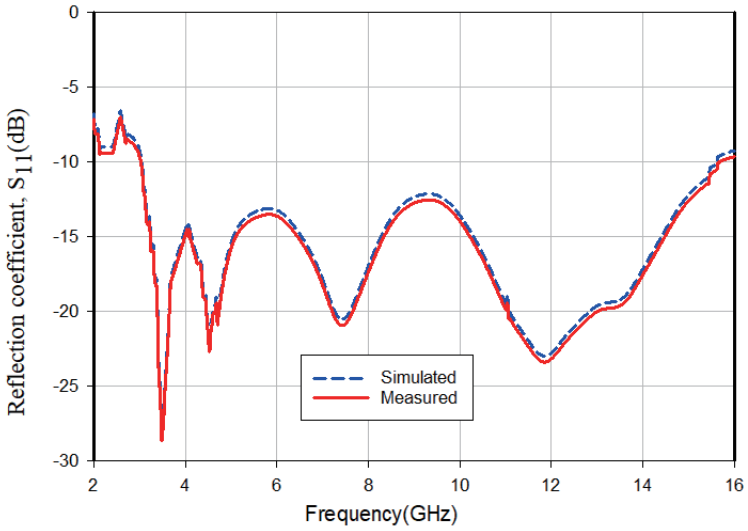

FIGURE 9. Simulated and measured reflection coefficient versus frequency plot of the CTWA.

3. EXPERIMENTAL RESULTS AND DISCUSSION

3.1. Fabrication of the CTWA

The proposed CTWA with the specifications mentioned in Table 1 is fabricated on a uniform, denim jeans substrate with a permittivity $\epsilon_r = 1.77$ and loss tangent $(\tan\delta) = 0.03034$. The overall dimension of the CTWA is 27 mm × 28 mm × 0.7 mm. As the substrate is a jeans material, extreme care is taken while soldering, so that it does not get burned. The semi-circular slotted elliptical patch, feed line, and ground plane are made of a self adhesive copper tape with nonconductive glue. The thickness of the copper tape used is 0.035 mm. For performing the experiment, a 50 Ω microstrip feed line is connected to an SMA connector. Fig. 8 shows the front and rear views of the fabricated CTWA. The reflection coefficient characteristics of the fabricated CTWA are measured using the vector network analyser Agilent PNAE8362B. Fig. 9 shows the plot of the simulated and measured reflection coefficients of the proposed CTWA. The measured bandwidth of CTWA is from 3.01 to 15.98 GHz. On comparing the results it can be seen that the simulated and experimental results of the CTWA are in close agreement.

3.2. Radiation Characteristics, Gain and Efficiency of the CTWA

The radiation characteristics of the CTWA are measured in an anechoic chamber as shown in Fig. 10. The measured co-polarization and cross polarization radiation patterns of the proposed CTWA in both the E plane and H plane for the frequencies 3.4 GHz, 7.3 GHz, and 11.8 GHz are shown in Fig. 11 and Fig. 12, respectively. From the radiation patterns, it can be seen that the patterns are omnidirectional as required for on-body WBAN applications. The radiation efficiency of the CTWA is measured using the Wheeler cap method [28]. In this method, the input resistances of the CTWA $(R_R + R_L)$ outside the metal cap (free space) and inside the metal cap (R_R) are measured using the vector network analyser. The efficiency of the proposed antenna is calculated using the expression.

$$E = \frac{R_R}{R_R + R_L} \tag{1}$$

FIGURE 10. Radiation pattern measurement setup.

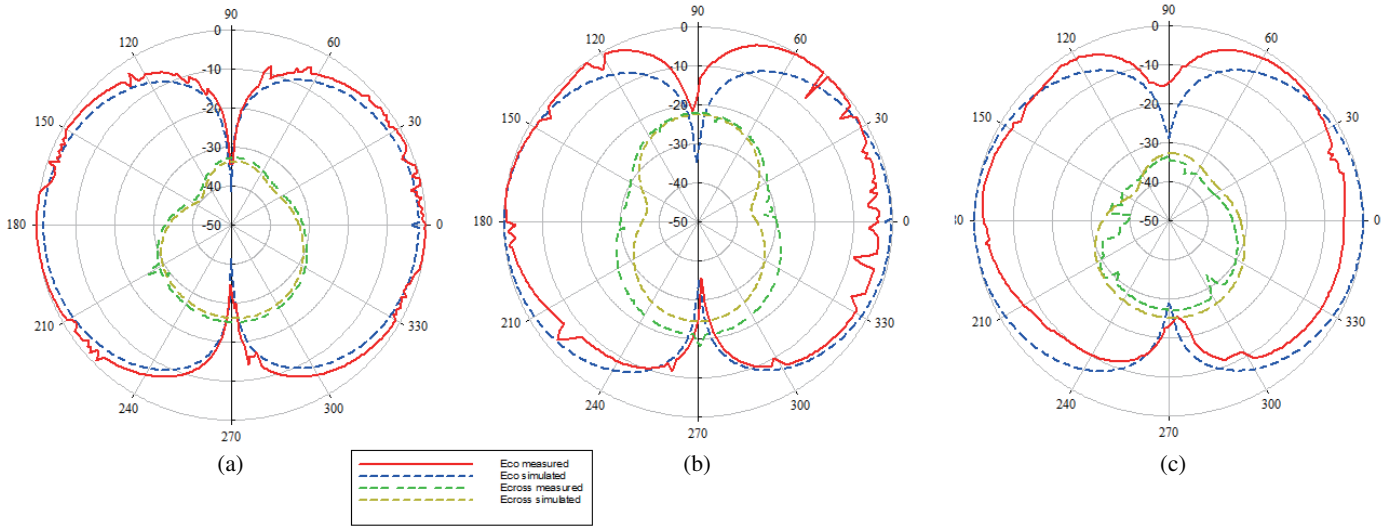

FIGURE 11. Measured and simulated radiation pattern of the CTWA along the E plane at (a) 3.4 GHz (b) 7.3 GHz (c) 11.8 GHz.

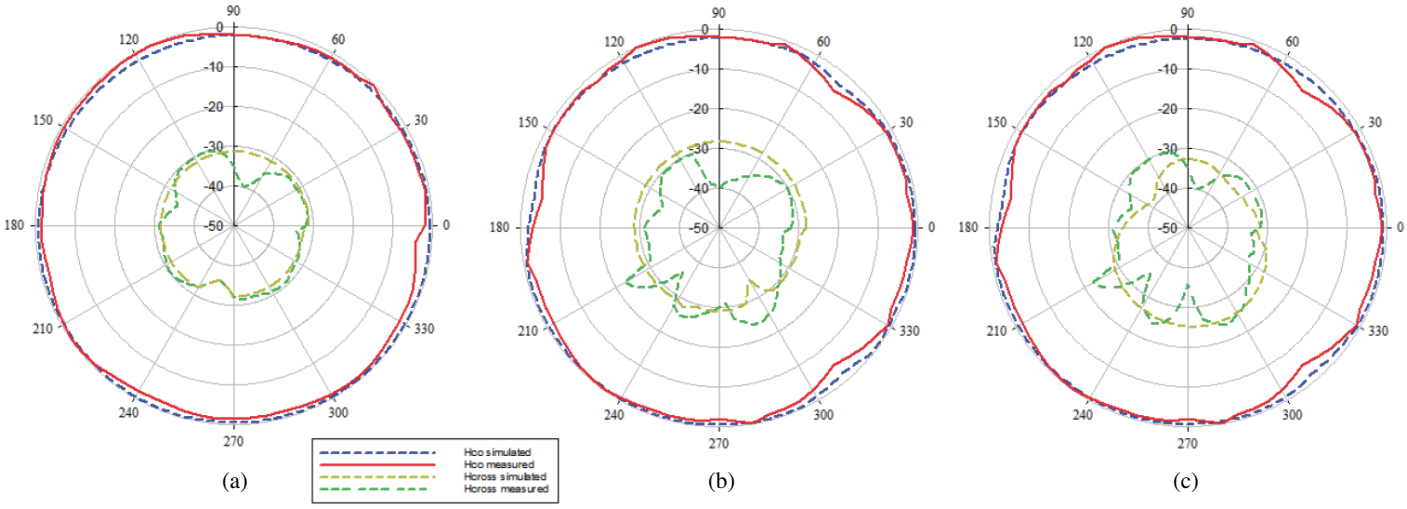

FIGURE 12. Measured and simulated radiation pattern of CTWA along H plane at (a) 3.4 GHz (b) 7.3 GHz (c) 11.8 GHz.

FIGURE 13. (a) Measurement set up for radiation efficiency of the proposed CTWA.

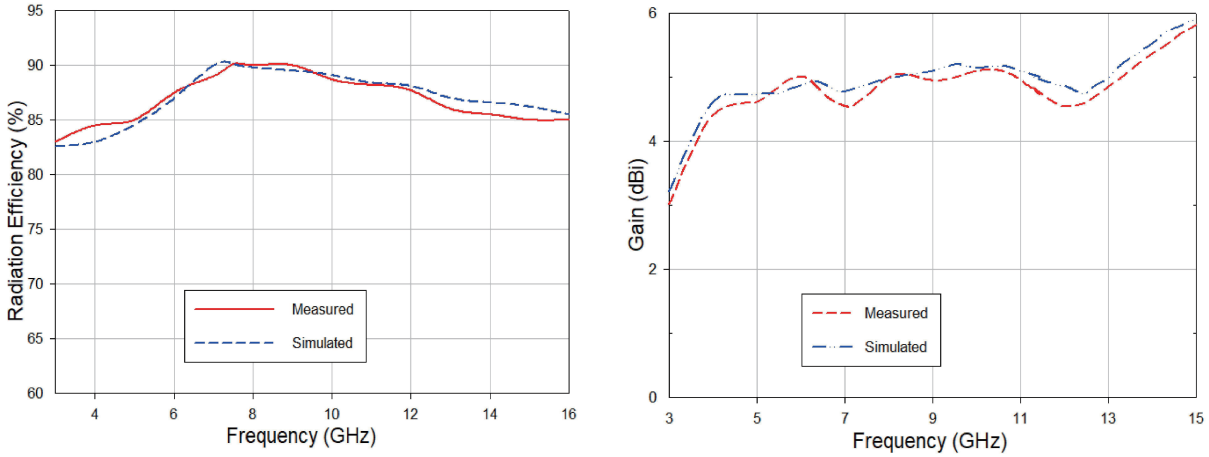

(a) (b)

FIGURE 14. (a) Radiation efficiency of the proposed CTWA. (b) Gain of the proposed CTWA.

Figures 13 and 14 show the measurement setup and radiation efficiency of the CTWA, respectively. The obtained radiation efficiency lies between 83.5 and 90.11% in the UWB. The gain measurements of the CTWA are carried out using the gain comparison method. The standard horn antenna is used for the gain comparison, and the resultant gain plot obtained is as shown in Fig. 14. The measured gain value varies from 2.98 to 5.81 dBi within the relevant band and hence makes it suitable for on-body wearable applications.

3.3. Bending Analysis

In the case of on-body WBAN applications, wearable antennas are subjected to different levels of bending while in use on the human body. The antenna's general characteristics and operating frequencies should not be affected when it is bent. Therefore in order to verify whether the proposed antenna gives a stable performance, structural deformation studies need to be carried out. Before loading the CTWA on a human body, free space deformation studies on convex and concave cylindrical surfaces with different radii in both horizontal (along x axis) and vertical (along y axis) directions are carried out. The cylindrical foams of ϵ_r close to 1 (air) are chosen for performing the free space bending analysis. The radii of the cylindrical foams are limited between 10 mm and 35 mm. Since the average wrist radius of a newborn baby is 20 mm, bending analysis with foam radius less than 10 mm is not carried out. Similarly, bending analysis beyond 35 mm is not carried out as the observed antenna characteristics with (on a 35 mm foam cylinder) and without bending are the same. In the real time scenarios, convex bending may happen if the antenna is placed on wrist, forearm, etc., and concave bending may happen if the antenna is placed in the knee pit, arm pit, etc. Foams of radii $R = 10$, 25, 30, and 35 mm are used to perform convex bending analysis, and the foams of radii $R = 10$, 25, and 35 mm are considered to perform concave bending analysis. Fig. 15 shows the placement of the antenna in the x and y directions over the foam of

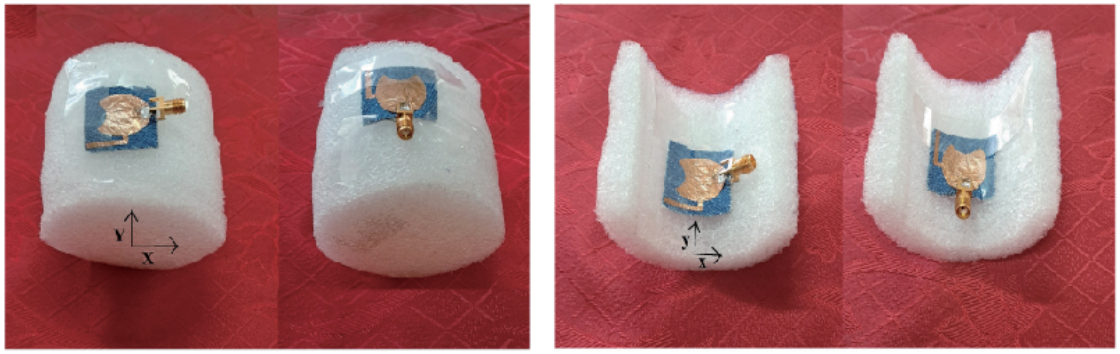

(a) (b)

FIGURE 15. Bending of the CTWA (x and y axis) on (a) convex surface (b) concave surface.

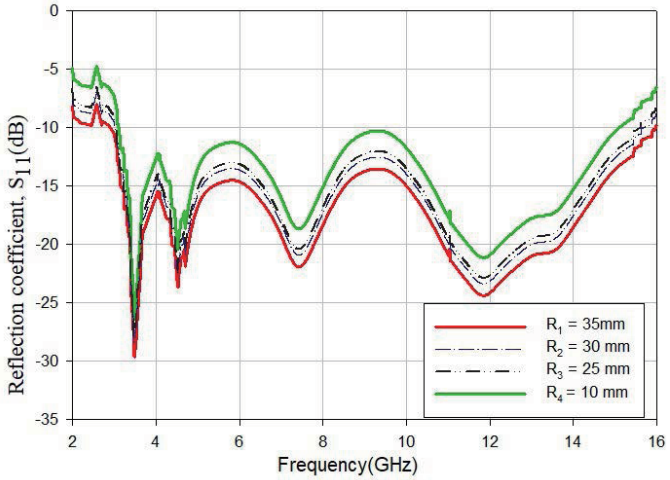

FIGURE 16. Reflection characteristics of the proposed CTWA on the convex surface (x bending).

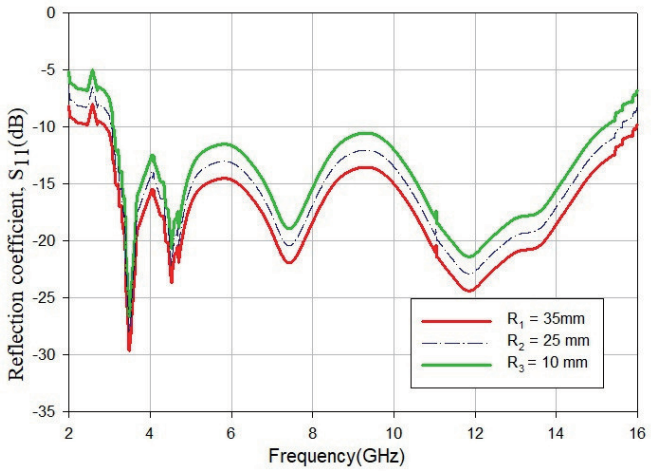

FIGURE 17. Reflection characteristics of the proposed CTWA on the concave surface (x bending).

radius 30 mm on both the convex and concave surfaces. An adhesive tape is used for fixing the antenna on the foam cylinders.

The reflection coefficient characteristics of the CTWA, when the antenna is bent along x axis on the convex and concave surfaced foam cylinders of different radii are shown in the Fig. 16 and Fig. 17, respectively. From the reflection coefficient characteristics, it is observed that while the antenna is bent along the x axis on convex and concave surfaces, the lower bound of the band shifted from 3.01 (at $R = 35$ mm) to 3.1 GHz (at $R = 10$ mm), and the upper bound shifted from 15.98 (at $R = 35$ mm) to 15.09 GHz (at $R = 10$ mm). Similarly in the case of concave x axis bending, the lower bound of frequency shifted from 3.01 GHz (at $R = 35$ mm) to 3.05 GHz (at $R = 10$ mm), and the upper bound shifted from 15.98 GHz (at $R = 35$ mm) to 15.2 GHz (at $R = 10$ mm). From the reflection coefficient characteristics, it is seen that although slight reduction in the reflection coefficient occurs, the UWB (3.1 to 10.6 GHz) behaviour of CTWA is preserved. In the same way, the reflection coefficient characteristics of the CTWA, when the antenna is bent along y axis on the convex and concave surfaced foam cylinders of different radii are as shown in Figs. 18 and 19, respectively. When the CTWA is bent along the y axis on convex surfaces, the lower bound of the band shifted from 3.01 (at $R = 35$ mm) to 2.8 GHz (at $R = 10$ mm), and the upper bound shifted from 15.98 (at $R = 35$ mm) to 15.63 GHz (at $R = 10$ mm). Similarly, when CTWA is bent along y axis on concave surfaces of different radii, the lower bound of frequency shifted slightly from 3.01 (at $R = 35$ mm) to 2.98 GHz (at $R = 10$ mm), and the upper bound of operating frequency shifted from 15.98 (at $R = 35$ mm) to 15.96 GHz (at $R = 10$ mm). From the reflection coefficient characteristics, it is seen that although the bandwidth of CTWA is shifted slightly, its UWB (3.1 to 10.6 GHz) behaviour is preserved. These changes in the case of x and y bending may be due to the changes that occur in the resonance length of the antenna when it is placed on the foams of different radii. Next, the analyses of the radiation characteristics of the CTWA under x and y bending conditions are carried out. The proposed antenna is placed on the concave and convex surfaced foam cylinders of different radii, and the corresponding E and H plane patterns are measured. The measured E plane patterns in the case of

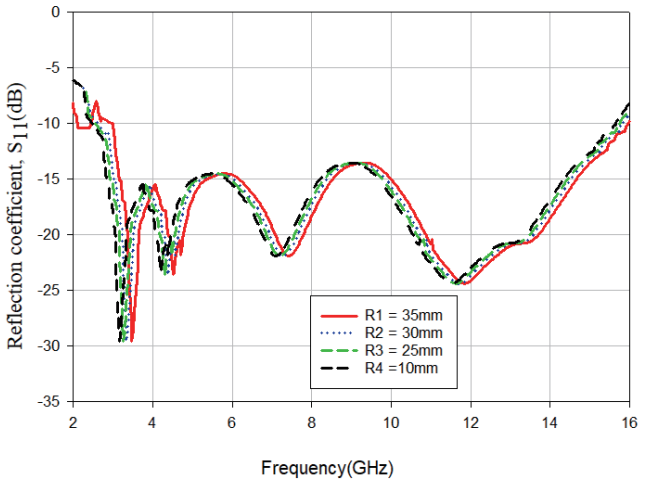

FIGURE 18. Reflection coefficient characteristics of the proposed CTWA on convex surface (y bending).

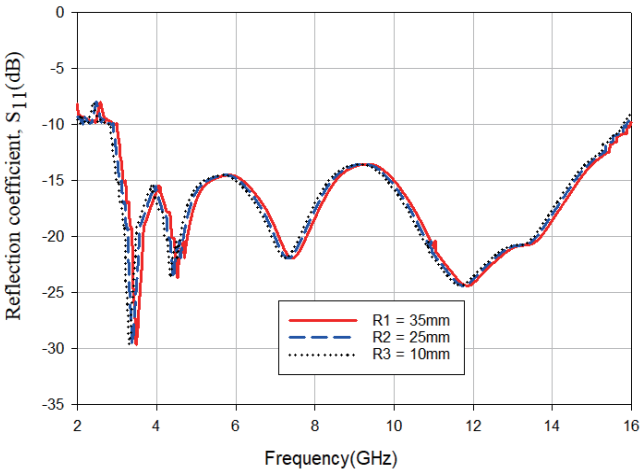

FIGURE 19. Reflection coefficient characteristics of the proposed CTWA on concave surface (y bending).

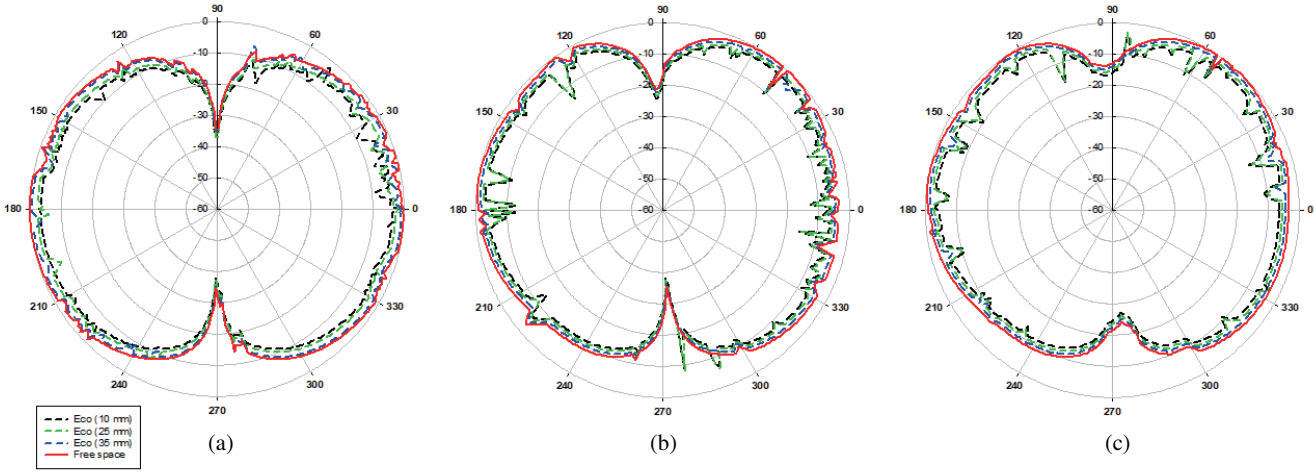

FIGURE 20. Convex bending-measured E plane patterns of the CTWA on different foam cylinders at the frequencies. (a) 3.4 GHz (b) 7.3 GHz (c) 11.8 GHz.

x bending and the H plane patterns in the case of y bending on convex surfaces of different radii are as shown in Figs. 20 and 21, respectively. Similarly, the measured E plane patterns in the case of x bending and H plane patterns in the case of y bending on concave surfaces of different radius are as shown in Figs. 22 and 23, respectively. From these experimental results it can be seen that in the case of both the concave and convex bending along the x and y axes, the radiation pattern is less affected, exhibiting a stable performance. The omnidirectional patterns show that the proposed antenna is suitable for on-body wearable applications.

3.4. Human Body Loading of the CTWA

In wearable WBAN applications, antennas are conformed to the human body surfaces in use. Thus, the performance of the CTWA, when it is placed on the human body needs to be studied. For this purpose, the CTWA is placed along the x and y axes on the different parts of the body like shoulder, elbow pit, and thigh of a female human volunteer of weight 65 kg and height 166 m as shown in Figs. 24 and 25, respectively.

The plot of the reflection coefficient when the CTWA is bent horizontally by placing the antenna on the different locations of the human body is shown in Fig. 26. Similarly, Fig. 27 portrays the reflection coefficient plot when the CTWA is bent along the y axis on the different human body spots.

From these x and y axis bending plots it is seen that, when the antenna is placed along the shoulder of the volunteer, the plot is similar to that of the reflection coefficient plot of the antenna without bending. However when it is placed in the elbow pit, a slight shift in the operating bandwidth is seen. These slight shifts may be due to the lossy nature of the human body and the changes in the resonant length of the antenna when it is bent. But in all these cases, the UWB behaviour of the CTWA is preserved. From these bending results, it is clear that the functions of the CTWA are unaffected while it is placed on a human body.

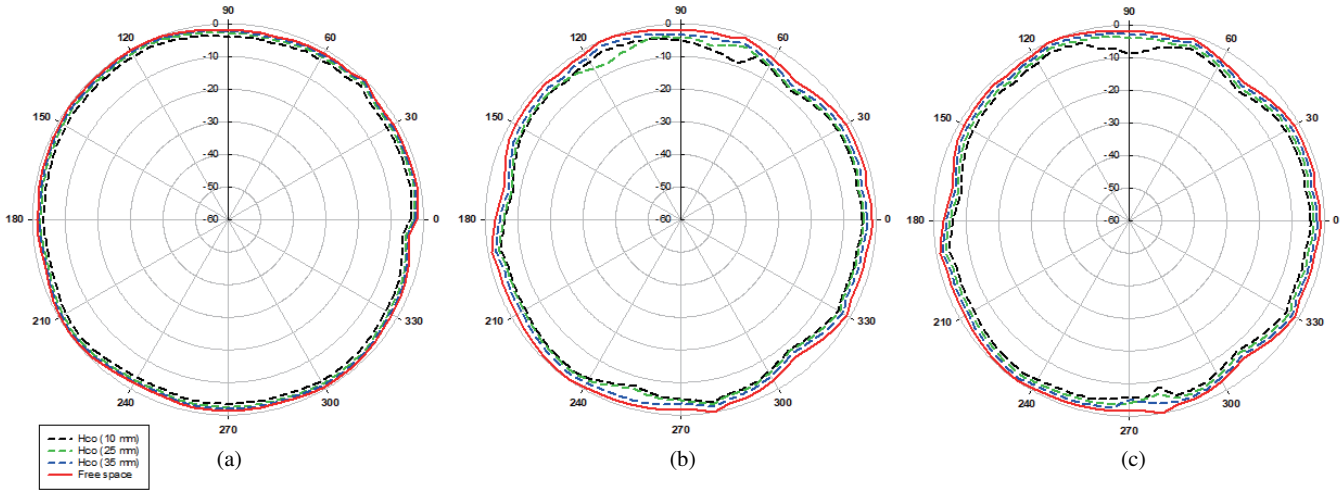

FIGURE 21. Convex bending-measured H plane patterns of the CTWA on different foam cylinders at the frequencies. (a) 3.4 GHz (b) 7.3 GHz (c) 11.8 GHz.

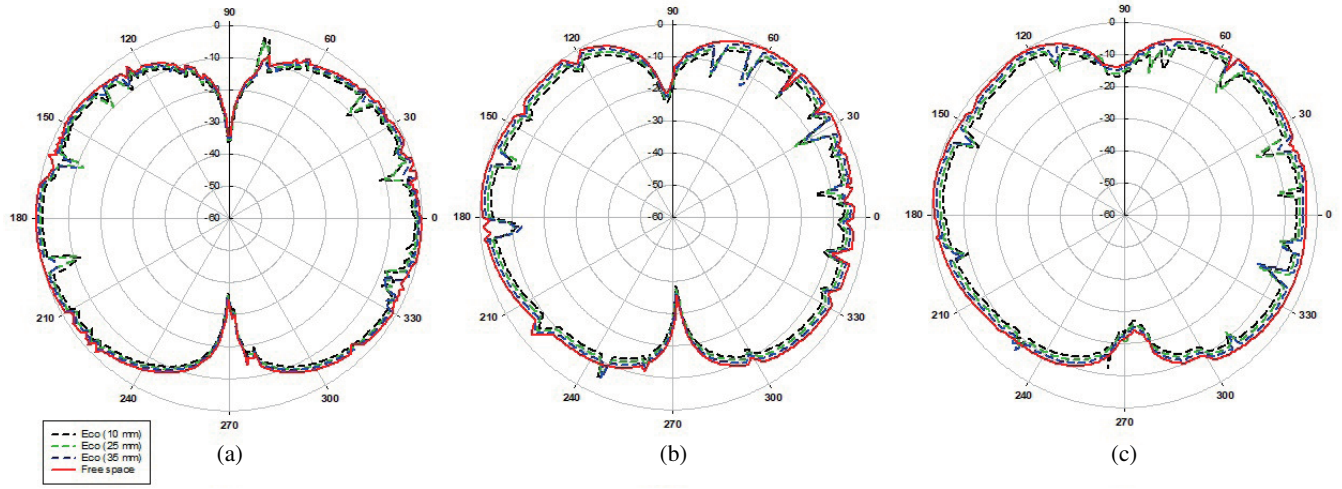

FIGURE 22. Concave bending-measured E plane patterns of the CTWA on different foam cylinders at the frequencies (a) 3.4 GHz (b) 7.3 GHz (c) 11.8 GHz.

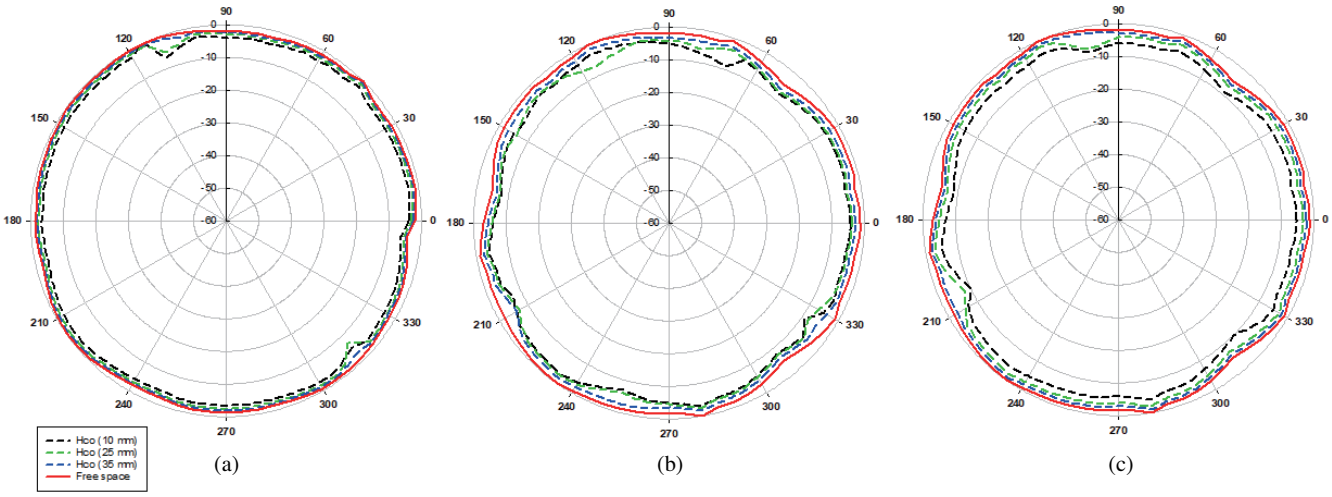

FIGURE 23. Concave bending-measured H plane patterns of the CTWA on different foam cylinders at the frequencies (a) 3.4 GHz (b) 7.3 GHz (c) 11.8 GHz.

(a) (b) (c)

FIGURE 24. The CTWA on the human body (x axis bending) (a) shoulder (b) elbow pit (c) thigh.

(a) (b) (c)

FIGURE 25. The CTWA on the human body (y axis bending) (a) shoulder (b) elbow pit (c) thigh.

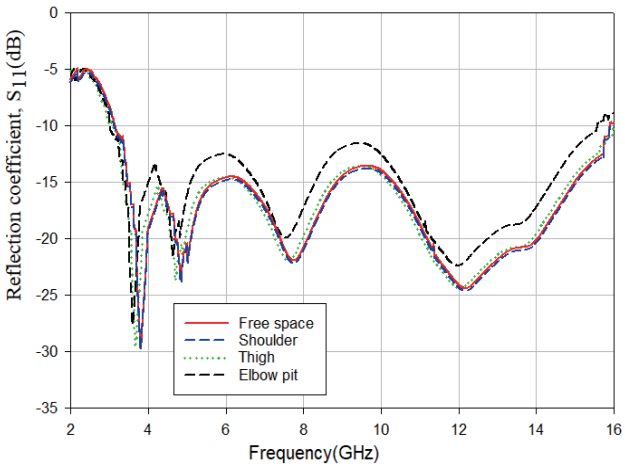

FIGURE 26. The CTWA at different places in the human body (x axis bending).

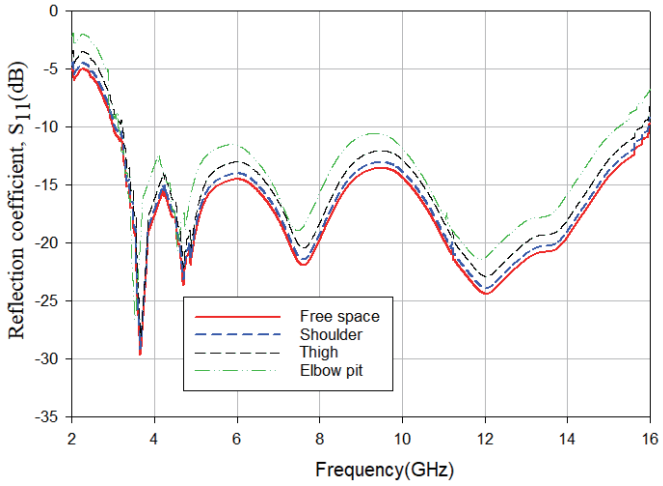

FIGURE 27. The CTWA on different surfaces of human body (y axis bending).

3.5. SAR Analysis of the Proposed CTWA

Wearable textile antenna can affect the human body when it is operated in the vicinity of the human beings. In order to investigate the effect of radiation on the human body, the specific absorption rate (SAR) of the proposed CTWA needs to be calculated. SAR is the rate of energy absorbed by the human body when it is exposed to a specific amount of electromagnetic radiation. The SAR value of a CTWA is computed on the rectangular human body model comprising skin, fat, and muscle as shown in Fig. 28(a). The thicknesses of the skin, fat, and muscle layers are chosen to be 1.7 mm, 8 mm, and 10 mm, respectively [29]. The modeled geometry is of the dimension 120 mm $\times$ 120 mm $\times$ 19.7 mm. An input power of 0.5 W as per the IEEE C95.3 standard is used for SAR calculations. The ma-

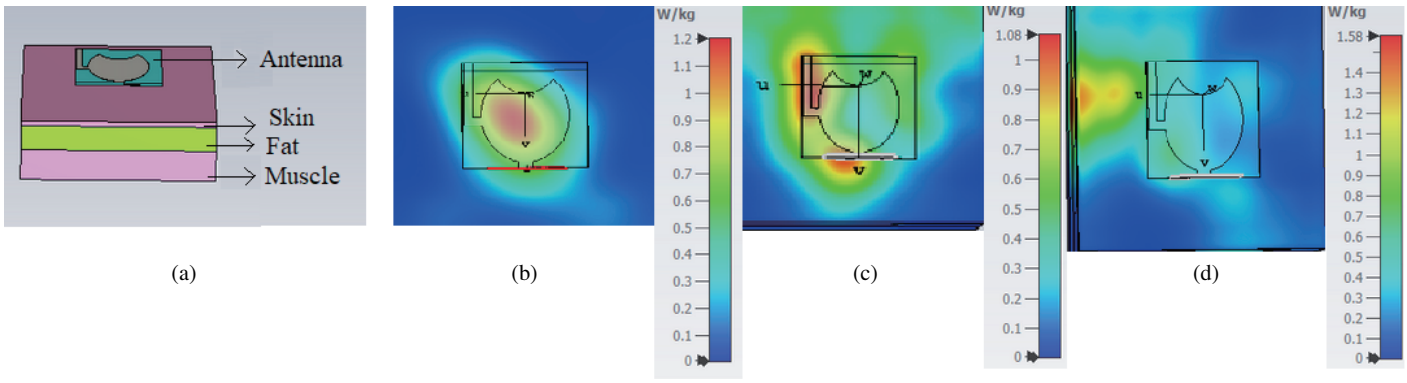

(a) (b) (c) (d)

FIGURE 28. SAR of the proposed CTWA. (a) human body model, (b) 4 GHz, (c) 7 GHz and (d) 10 GHz.

(a) (b) (c)

FIGURE 29. Group delay measurements: (a) Face to face (b) face to side (c) side to side.

TABLE 2. Material density and dielectric constant values of the human body tissues used in the simulations.

Tissue	Density	Dielectric constant (4 GHz)	Dielectric constant (7.5 GHz)	Dielectric constant (10.5 GHz)
Skin	1100	35.3	30.6	28.4
Fat	910	5.1	4.6	4.4
Muscle	1041	50	43.3	38.3

terial density and dielectric constant values of the human body tissues used in the simulations are given in Table 2.

The SAR values calculated for the proposed CTWA for frequencies 4, 7, and 10 GHz are 1.2, 1.06, and 1.58 W/Kg, respectively, and are shown in Fig. 28. It can be seen that the results are within the FCC limit.

3.6. Group Delay

Group delay is a measure of the negative derivative of the phase with respect to frequency. The group delay of a CTWA is measured using a network analyser. Two CTWAs (proposed) are placed at a far field distance of 12 cm from each other in three orientations (face to face, face to side, and side to side) as shown in Fig. 29. Fig. 30 shows the group delay characteristics of the CTWA. The maximum group delay of proposed CTWA in the UWB is 0.22 ns which is within the acceptable limit of 1 ns [41, 42].

3.7. Performance Comparison

The performances of the CTWA in terms of fractional bandwidth, efficiency, gain, SAR, etc. are compared with notable UWB wearable antennas available in the literature. Table 3 shows the comparative evaluation of the CTWA. The comparative evaluation highlights that the proposed CTWA has a low profile and high fractional bandwidth of 137% compared to the other similar works in the literature. Moreover, the CTWA offers a high efficiency of 90.11% and maximum gain of 5.81 dBi with adequate bending performance and an acceptable SAR.

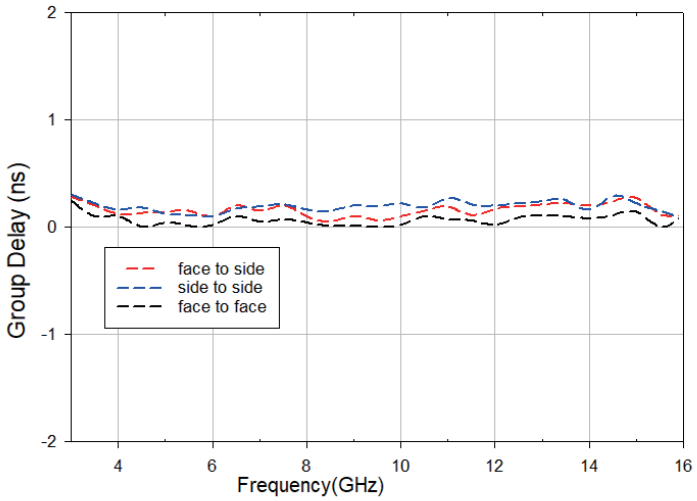

FIGURE 30. Group delay characteristics of the CTWA.

TABLE 3. Comparative evaluation of the CTWA.

Ref. (Year)	Size	Frequency Range	Fractional Bandwidth	Efficiency (%) (max)	Gain (max)	Fabric	SAR analysis	bending analysis
[30] (2023)	84 mm × 69 mm × 3.4 mm	4.6 GHz–10.1 GHz	75%	73	7.2 dBi	PF-4 foam	yes	yes
[31] (2016)	80 mm × 61 mm × 4.51 mm	3.1 GHz–10.6 GHz	109%	NA	7.2 dBi	felt	yes	no
[32] (2014)	30 mm × 40 mm × 0.75 mm	3 GHz–12 GHz	120%	80	4 dBi	cotton	no	yes
[33] (2021)	30 mm × 30 mm × 0.7 mm	3.1 GHz–11.3 GHz	114%	60	4 dBi	felt	no	yes
[34] (2021)	40 mm × 42 mm × 2 mm	2.8 GHz–10.9 GHz	118%	98	NA	jeans	no	no
[35] (2021)	36 mm × 29 mm × 2 mm	3 GHz–11 GHz	114%	NA	NA	jeans	no	no
[36] (2019)	39 mm × 42 mm × 3.34 mm	6.5 GHz–9.9 GHz	34%	NA	5.67	felt	yes	yes
[37] (2023)	38 mm × 30 mm × 1.7 mm	2.6 GHz–11.3 GHz	125%	NA	5.24 dBi	foam	yes	yes
[38] (2021)	30 mm × 35 mm × 1.2 mm	3.2 GHz–11.8 GHz	115%	NA	4.63 dBi	jeans	no	yes
[39] (2022)	60 mm × 60 mm × 1.38 mm	3.1 GHz–10.6 GHz	109%	88	4.5 dBi	felt	no	yes
[40] (2014)	88 mm × 97 mm × 3 mm	3.4 GHz–10.2 GHz	100%	NA	7.75 dBi	felt	no	no
Proposed	**27 mm × 28 mm × 0.7 mm**	**3.01 GHz–15.98 GHz**	**137%**	**90.11**	**5.81 dBi**	**jeans**	**yes**	**yes**

4. CONCLUSION

In this work, an Ultra Wide Band-Compact Textile Wearable Antenna (UWB-CTWA) suitable for Wireless Body Area Network applications is presented. Its suitability is experimentally verified and found adequate. The proposed CTWA shows high radiation efficiency (83.5%–90.11%) in the whole working band (3.01–15.98 GHz). The overall dimension of the antenna is 27 mm × 28 mm × 0.7 mm, and it has a high fractional bandwidth of 137%. The gain of the CTWA ranges from 2.98 dBi to 5.81 dBi, and its SAR value is within the FCC limit. The structural deformation studies on the convex and concave surfaces of the human body are carried out, and the performance of the proposed CTWA is found to be stable. The advantages of the proposed CTWA like compactness, ease of availability of substrate, repeatability, flexibility, high fractional bandwidth, high efficiency, gain, and omnidirectional radiation pattern make it an appropriate candidate for on-body wearable wireless body area network.

ACKNOWLEDGEMENT

The authors would like to thank Dr.Deepthi Das Krishna, Associate professor and Neema K, Research scholar at the Centre For Research In Electromagnetics and Antennas (CREMA), Cochin university of science and technology for extending the measurement facilities.

REFERENCES

[1] Hall, P. S. and Y. Hao, *Antennas and Propagation For Body-Centric Wireless Communications*, Artech House, 2012.

[2] Meharouech, A., J. Elias, and A. Mehaoua, "Moving towards body-to-body sensor networks for ubiquitous applications: A survey," *Journal of Sensor and Actuator Networks*, Vol. 8, No. 2, 27, 2019.

[3] Mukhopadhyay, S. C., "Wearable sensors for human activity monitoring: A review," *IEEE Sensors Journal*, Vol. 15, No. 3, 1321–1330, 2014.

[4] Abbasi, Q. H., M. U. Rehman, K. Qaraqe, and A. Alomainy, *Advances in Body-Centric Wireless Communication: Applications*

and State-of-the-art, Institution of Engineering and Technology, 2016.

[5] Corchia, L., G. Monti, and L. Tarricone, "Wearable antennas: Nontextile versus fully textile solutions," *IEEE Antennas and Propagation Magazine*, Vol. 61, No. 2, 71–83, 2019.

[6] El Maleky, O., F. B. Abdelouahab, M. Essaaidi, and M. A. Ennasar, "Design of simple printed Dipole antenna on flexible substrate for UHF band," *Procedia Manufacturing*, Vol. 22, 428–435, 2018.

[7] Khaleel, H. R., H. M. Al-Rizzo, D. G. Rucker, and S. Mohan, "A compact polyimide-based UWB antenna for flexible electronics," *IEEE Antennas and Wireless Propagation Letters*, Vol. 11, 564–567, 2012.

[8] Jain, S., P. K. Mishra, V. V. Thakare, and J. Mishra, "Design and analysis of moisture content of hevea latex rubber using microstrip patch antenna with DGS," *Materials Today: Proceedings*, Vol. 29, 556–560, 2020.

[9] Cang, D., Z. Wang, and H. Qu, "A polyimide-based flexible monopole antenna fed by a coplanar waveguide," *Electronics*, Vol. 10, No. 3, 334, 2021.

[10] Arif, A., M. Zubair, M. Ali, M. U. Khan, and M. Q. Mehmood, "A compact, low-profile fractal antenna for wearable on-body WBAN applications," *IEEE Antennas and Wireless Propagation Letters*, Vol. 18, No. 5, 981–985, 2019.

[11] Cabrol, P. and P. Pietraski, "60 GHz patch antenna array on low cost Liquid-Crystal Polymer (LCP) substrate," in *IEEE Long Island Systems, Applications and Technology (LISAT) Conference 2014*, 1–6, IEEE, 2014.

[12] Mahmood, S. N., A. J. Ishak, T. Saeidi, H. Alsariera, S. Alani, A. Ismail, and A. C. Soh, "Recent advances in wearable antenna technologies: A review," *Progress In Electromagnetics Research B*, Vol. 89, 1–27, 2020.

[13] Koul, S. K. and R. Bharadwaj, *Wearable Antennas and Body Centric Communication: Present and Future*, Springer Nature, 2021.

[14] Kumar, O. P., P. Kumar, T. Ali, P. Kumar, and S. Vincent, "Ultrawideband antennas: Growth and evolution," *Micromachines*, Vol. 13, No. 1, 60, 2021.

[15] Varkiani, S. M. H. and M. Afsahi, "Compact and ultra-wideband CPW-fed square slot antenna for wearable applications," *AEU — International Journal of Electronics and Communications*, Vol. 106, 108–115, 2019.

[16] Lakrit, S., S. Das, B. Madhav, and K. V. Babu, "An octagonal star shaped flexible UWB antenna with band-notched characteristics for WLAN applications," *Journal of Instrumentation*, Vol. 15, No. 02, P02021, 2020.

[17] Yahya, R., M. R. Kamarudin, and N. Seman, "Effect of rainwater and seawater on the permittivity of denim jean substrate and performance of UWB eye-shaped antenna," *IEEE Antennas and Wireless Propagation Letters*, Vol. 13, 806–809, 2014.

[18] Shikder, K. and F. Arifin, "Design and evaluation of a UWB wearable textile antenna for body area network," in *2015 2nd International Conference on Electrical Information and Communication Technologies (EICT)*, 326–330, IEEE, 2015.

[19] Zeouga, K., L. Osman, A. Gharsallah, and B. Gupta, "Truncated patch antenna on jute textile for wireless power transmission at 2.45 GHz," *International Journal of Advanced Computer Science and Applications*, Vol. 9, No. 1, 2018.

[20] Hosseini Varkiani, S. M. and M. Afsahi, "Grounded CPW multiband wearable antenna for MBAN and WLAN applications," *Microwave and Optical Technology Letters*, Vol. 60, No. 3, 561–568, 2018.

[21] De, A., B. Roy, A. Bhattacharya, and A. Bhattacharjee, "Investigations on a circular UWB antenna with Archimedean spiral slot for WLAN/Wi-MAX and satellite X-band filtering feature," *International Journal of Microwave and Wireless Technologies*, Vol. 14, No. 6, 781–789, 2022.

[22] Raj, S., P. K. Mishra, S. Tripathi, and V. S. Tripathi, "A defected ground structure based compact circular patch antenna design for mm-Wave application," *Defence Science Journal*, Vol. 72, No. 4, 2022.

[23] Del-Rio-Ruiz, R., J.-M. Lopez-Garde, and J. Legarda, "Planar textile off-body communication antennas: A survey," *Electronics*, Vol. 8, No. 6, 714, 2019.

[24] Gupta, V. K. and A. Gupta, "Design of an aperture coupled MIMO antenna for on-body communication and performance enhancement with dielectric back reflector," *Frequenz*, Vol. 75, 1–2, 2021.

[25] Yin, B., J. Gu, X. Feng, B. Wang, Y. Yu, and W. Ruan, "A low SAR value wearable antenna for wireless body area network based on AMC structure," *Progress In Electromagnetics Research C*, Vol. 95, 119–129, 2019.

[26] Razavi, S. A., *Bandwidth Enhancement Techniques*, INTECH Open, 2017.

[27] Wang, C.-J. and Y.-L. Lee, "A compact dipole antenna for DTV applications by utilizing L-shaped stub and coupling strip," *IEEE Transactions on Antennas and Propagation*, Vol. 62, No. 12, 6515–6519, 2014.

[28] Chair, R., K. M. Luk, and K. F. Lee, "Radiation efficiency analysis on small antenna by wheeler cap method," *Microwave and Optical Technology Letters*, Vol. 33, No. 2, 112–113, 2002.

[29] Yalduz, H., T. E. Tabaru, V. T. Kilic, and M. Turkmen, "Design and analysis of low profile and low SAR full-textile UWB wearable antenna with metamaterial for WBAN applications," *AEU — International Journal of Electronics and Communications*, Vol. 126, 153465, 2020.

[30] Samal, P. B., S. J. Chen, and C. Fumeaux, "Wearable textile multiband antenna for WBAN applications," *IEEE Transactions on Antennas and Propagation*, Vol. 71, No. 2, 1391–1402, 2022.

[31] Poffelie, L. A. Y., P. J. Soh, S. Yan, and G. A. E. Vandenbosch, "A high-fidelity all-textile UWB antenna with low back radiation for off-body WBAN applications," *IEEE Transactions on Antennas and Propagation*, Vol. 64, No. 2, 757–760, 2016.

[32] Sun, Y., S. W. Cheung, and T. I. Yuk, "Design of a textile ultra-wideband antenna with stable performance for body-centric wireless communications," *IET Microwaves, Antennas & Propagation*, Vol. 8, No. 15, 1363–1375, 2014.

[33] El Gharbi, M., M. Martinez-Estrada, R. Fernández-García, S. Ahyoud, and I. Gil, "A novel ultra-wide band wearable antenna under different bending conditions for electronic-textile applications," *The Journal of The Textile Institute*, Vol. 112, No. 3, 437–443, 2021.

[34] Parameswari, S. and C. Chitra, "Compact textile UWB antenna with hexagonal for biomedical communication," *Journal of Ambient Intelligence and Humanized Computing*, 1–8, 2021.

[35] Parameswari, S. and C. Chitra, "Textile UWB antenna with metamaterial for healthcare monitoring," *International Journal of Antennas and Propagation*, Vol. 2021, 1–11, 2021.

[36] Samal, P. B., P. J. Soh, and Z. Zakaria, "Compact microstrip-based textile antenna for 802.15.6 WBAN-UWB with full ground plane," *International Journal of Antennas and Propagation*, Vol. 2019, 1–12, 2019.

[37] Karad, K. V. and V. S. Hendre, "A flower bud-shaped flexible UWB antenna for healthcare applications," *EURASIP Journal on Wireless Communications and Networking*, Vol. 2023, No. 1,

1–18, 2023.

[38] Tiwari, B., S. H. Gupta, and V. Balyan, "Investigation on performance of wearable flexible on-body ultra-wideband antenna based on denim for wireless health monitoring," *Journal of Electronic Materials*, Vol. 50, 6897–6909, 2021.

[39] Rambe, A. H., M. Jusoh, S. S. Al-Bawri, and M. A. Abdelghany, "Wearable UWB antenna-based bending and wet performances for breast cancer detection," *Computers, Materials and Continua*, Vol. 73, No. 3, 5575–5587, 2022.

[40] Samal, P. B., P. J. Soh, and G. A. E. Vandenbosch, "UWB all-textile antenna with full ground plane for off-body WBAN communications," *IEEE Transactions on Antennas and Propagation*, Vol. 62, No. 1, 102–108, 2014.

[41] Yadav, A., V. K. Singh, A. K. Bhoi, G. Marques, B. Garcia-Zapirain, and I. de la Torre Díez, "Wireless body area networks: UWB wearable textile antenna for telemedicine and mobile health systems," *Micromachines*, Vol. 11, No. 6, 558, 2020.

[42] Jayakumar, S. and G. Mohanbabu, "A wearable low profile asymmetrical slotted ultra-wide band antenna for WBAN applications," *EURASIP Journal on Wireless Communications and Networking*, Vol. 2022, No. 1, 103, 2022.